Journal of Drug Delivery Science and Technology 101 (2024) 106169

Contents lists available at ScienceDirect

Journal of Drug Delivery Science and Technology

journal homepage: www.elsevier.com/locate/jddst

Self-assembling nanoparticles for miRNA delivery towards precision medicine against melanoma

Valeria Nele [a], Domenico Liguoro [b], Virginia Campani [c], Alessia Angelillo [a], Rachele Frigerio [d], Arianna Ortolano [e], Rita Mancini [f,g], Luigi Fattore [b,*], Giuseppe De Rosa [a,1], Gennaro Ciliberto [h,1]

[a] Department of Pharmacy, University of Naples Federico II, 80131, Naples, Italy
[b] SAFU Laboratory, Department of Research, Advanced Diagnostics and Technological Innovation, Translational Research Area, IRCCS Regina Elena National Cancer Institute, 00144, Rome, Italy
[c] Department of Life Health Sciences and Health Professions, Link Campus University, Rome, 00165, Italy
[d] Department of Experimental and Clinical Medicine, ''Magna Graecia'' University of Catanzaro, 88100, Catanzaro, Italy
[e] Department of Anatomy, Histology, Forensic- Medicine and Orthopedics, Sapienza University of Rome, 00161, Rome, Italy
[f] Department of Clinical and Molecular Medicine, Sapienza University of Rome, 00161, Rome, Italy
[g] Faculty of Medicine and Psychology, Department Clinical and Molecular Medicine, Sant'Andrea Hospital-Sapienza University of Rome, 00118, Rome, Italy
[h] Scientific Directorate, IRCSS Regina Elena National Cancer Institute, 00144, Rome, Italy

ARTICLE INFO

Keywords:
Self-assembling nanoparticles
microRNA
Metastatic melanoma
Lipid-based nanoparticles

ABSTRACT

Metastatic melanoma is a highly aggressive tumor with a poor prognosis. One of the therapeutic options for patients bearing BRAF V600E mutations is targeted therapy, which is based on the use of drugs able to inhibit the mitogen-activated protein kinase (MAPK) pathway. However, the long-term efficacy of targeted therapy is compromised by the onset of drug resistance. We previously identified a panel of oncosuppressor microRNAs (miRNAs) able to prevent the development of drug resistance to targeted therapy. We also developed self-assembling nanoparticles (SANP) as a promising and versatile nanomedicine platform for RNA-based personalized therapies. Here, we provide the proof-of-principle of a miRNA-based therapeutic strategy against BRAF-mutant melanomas. The role of the cationic lipid, ionizable lipid, cholesterol, and PEGylated lipid in SANP formulations was investigated to optimize miRNA encapsulation and delivery to melanoma cells. miRNA-loaded SANPs inhibited the release of soluble tumor-promoting factors and prevented the proliferation of metastatic melanoma cells. When used in combination with targeted therapy, miRNA-SANPs were able to potentiate its efficacy in a dose-response manner. These results pave the way for further studies on SANP as a platform for miRNA delivery to prevent the development of resistance to targeted therapy in metastatic melanoma.

1. Introduction

Metastatic melanoma is a highly aggressive tumor that can be fatal within 18 months of diagnosis [1]. Current therapeutic approaches comprise targeted therapy and immunotherapy [2,3]. Targeted therapy inhibits the activation of the mitogen-activated protein kinase (MAPK) pathway which drives melanoma proliferation and progression. The MAPK pathway is over-activated in patients with v-raf murine sarcoma viral oncogene homolog B1 (BRAF) V600 mutations occurring in approximately 50 % of cases [4]. Targeted therapy can greatly improve progression-free and overall survival rates compared to previous treatments [4], but its long-term efficacy is impaired by the development of drug resistance [4]. We have recently identified a panel of microRNAs (miRNAs) able to halt the development of resistance to MAPK inhibition therapy in BRAF-mutated melanoma [5] when used in combination with targeted therapy. MiRNAs are short (20–24 nucleotides), non-coding RNAs which regulate key cellular functions such as metabolism, differentiation, proliferation, and apoptosis [6] and have emerged as potential therapeutics for a wide range of applications [7].

Systemic delivery of miRNA poses several challenges associated to poor cellular uptake, off-target effects, and nuclease degradation, requiring the use of delivery system able to overcome these issues. Non-viral vectors for miRNA delivery comprise lipid nanoparticles (LNPs) and polymer nanoparticles [6,8]. The approval of Onpattro® (LNPs

* Corresponding author.
E-mail address: luigi.fattore@ifo.it (L. Fattore).
[1] these authors contributed equally.

https://doi.org/10.1016/j.jddst.2024.106169
Received 20 May 2024; Received in revised form 2 September 2024; Accepted 8 September 2024
Available online 12 September 2024

encapsulating a small interfering RNA) and of Comirnaty® and Spike-Vax® (LNPs encapsulating a messenger RNA) has dramatically accelerated the clinical adoption and scale-up manufacturing of nucleic acid-loaded LNPs. LNPs complex anionic nucleic acids with high encapsulation efficiencies and are promising nanovectors for miRNA delivery [9–12]. In this context, our group has recently demonstrated the therapeutic potential of LNPs encapsulating a combination of oncosuppressive miR-204–5p and miR-199b-5p to potentiate targeted therapy and to delay the emergence of drug resistance using various preclinical melanoma models *in vitro* and *in vivo* [13].

However, LNP formulations require RNA encapsulation at the nanoparticle manufacturing stage, which limits their applicability in the context of personalized medicine. Given the heterogeneity of melanoma [14], advancements in melanoma transcriptome profiling may be able to identify combinations of therapeutic miRNAs tailored to the individual patient or to subsets of patients in the near future. The rapid emergence of personalized medicine makes the development of a versatile nanoparticle platform enabling miRNA loading and delivery at the point of care of vital importance. In this context, core-shell nanoparticles with an inorganic or organic core enclosed by a lipid shell may be a promising approach. Example core materials comprise polypeptides, hyaluronic acid, chitosan, calcium phosphate (CaP), and synthetic polymers [15]. CaP cores complex negatively charged molecules such as miRNA and exhibit low cytotoxicity, ease of preparation, and pH-responsiveness. The calcium phosphate core dissolves in the acidic environment of the cellular endosomes and releases the payload in the cytosol [16,17].

We have pioneered the development of self-assembling nanoparticles with a CaP core (SANP). They can be prepared by mixing the CaP nanoparticles, the liposomes, and the payload; these components are colloidally stable, can be easily transported and stored at 4 °C for up to 1 year, and can be manufactured at industrial scales in GMP conditions using well-established protocols. The colloidal stability of the SANP components at 4 °C may also allow to overcome some of the challenges currently associated with LNPs, which suffer from payload degradation upon long-term storage and typically need to be stored at low temperatures. While SANP were originally developed for bisphosphonates delivery [18–21], we have recently demonstrated that these formulations can also be used to deliver microRNA for the treatment of glioblastoma [22] or endowed with the ability to scavenge reactive oxygen species [23,24]. These examples highlight the versatility of the SANP platform, which can be leveraged for a wide range of applications. Given their extemporaneous assembling approach, miRNA-SANP are well-suited for the development of personalized nanomedicines against melanoma which can be assembled at the point-of-care and are prone to a rapid bench-to-bedside translation.

SANP require the use of cationic lipids able to interact with the calcium phosphate core encapsulating the anionic miRNA and a PEGylated lipid to ensure nanoparticle stability against aggregation in complex fluids and in circulation. We also explored the effect of cholesterol and of an ionizable lipid, namely 1,2-dioleoyl-3-dimethylammonium-propane (DODAP), on the colloidal properties of the formulations and on their efficacy. Cholesterol was chosen due to its ability to improve the transfection efficiency of cationic liposomes [25,26], while DODAP was used in combination with DOTAP to explore its effect on miRNA intra-cellular delivery. Ionizable lipids exhibit a neutral charge at physiological pH and become positively charged at the acidic pH of the endosomal compartment, favoring the endosomal escape of the encapsulated payload [27]. Previous work on hybrid lipid-polymer nanoparticles loaded with a messenger RNA has demonstrated an improvement in the transfection efficiency when a cationic lipid was used in combination with an ionizable lipid [28].

We therefore designed SANP formulations with varying lipid composition to deliver a mixture of oncosuppressor miRNAs against BRAF-mutated metastatic melanoma. We characterized the miRNA-loaded SANP formulations in terms of colloidal properties, surface charge, miRNA encapsulation efficiencies, colloidal stability in serum, and haemolytic activity. We investigated the ability of selected SANP formulations to deliver miRNA, to inhibit the release of soluble tumor-promoting factors, and to prevent the proliferation of two different cell lines of metastatic melanoma. MiRNA-SANP formulations were then tested in combination with drugs used clinically for targeted therapy and investigated their synergic effect on cancer cell proliferation.

2. Materials and methods

2.1. Materials

Sodium chloride (NaCl), calcium chloride ($CaCl_2$), and sodium phosphate dibasic (Na_2HPO_4) were purchased from Merk Life Science S.r.l. (Milan, Italy). 1,2-dioleoyl-3-trimethylammonium-propane chloride (DOTAP) was kindly donated by Lipoid GmbH (Ludwigshafen, Germany) while N-palmitoylsphingosine-1 {succinyl[methoxy(polyethylene glycol)2000]} (Cer_{16}-PEG_{2000}), cholesterol, and 1,2-dioleoyl-3-dimethylammonium-propane (DODAP) were purchased from Avanti Polar Lipids (Alabaster, USA). Regenerated cellulose syringe filters with a 0.2 μm pore size were purchased from Exacta + Optech Labcenter SpA (San Prospero, Italy). Scramble miRNA (miR-scr, sequence: 5′-UUUAUGGUUCACCUAGCUUGC–3′), microRNA-199b-5p (miR199, sequence: 5′-CCCAGUGUUUAGACUAUCUGUUC-3′), and microRNA-204–5p (miR204, sequence: 5′-UUCCCUUUGUCAUCCUAUGCCU-3′) were purchased from Tema Ricerca s.r.l. (Bologna, Italy). The Quant-iT RiboGreen RNA Assay was purchased from ThermoFisher Scientific (Milan, Italy).

2.2. CaP nanoparticle synthesis

CaP nanoparticles were prepared by adding an aqueous solution of 10.8 mM Na_2HPO_4 (pH 9.5) to an aqueous solution of 18 mM $CaCl_2$ (pH 9.5) in a 1:1 v/v ratio dropwise while stirring at 1400 rpm. The CaP NPs suspension was left to stir for 10 min and filtered through 0.22 μm pore-sized polycarbonate filters. The CaP nanoparticle suspension was then stored at 4 °C until further use.

2.3. Liposome preparation

PEGylated liposomes were prepared by the thin film hydration method followed by extrusion. The lipids were dissolved in a chloroform:methanol mixture (2:1 v/v) and placed in a 50 mL round bottom flask. The organic solvent was removed by rotary evaporation (Laborata 4010 digital, Heidolph, Schwabach, Germany) and the obtained lipid film was hydrated with RNAse-free water for 2 h at 65 °C. The vesicle suspension was extruded through pore-sized polycarbonate membranes (Nucleopore Track-Etched 25 mm membrane, Whatman, Brentford, UK) by using a thermobarrel extruder (Lipex Extruder, Evonik, Essen, Germany) at 65 °C. More specifically, the vesicle suspension was forced to pass sequentially through 400 nm membranes (3 passages), 200 nm membranes (3 passages), and 100 nm membranes (5–7 passages depending on the lipid composition). The lipid composition used in this study are shown in Table 1.

2.4. SANP preparation

SANP formulations encapsulating miRNA were prepared by mixing a

Table 1
Lipid composition used in this study.

Formulation	DOTAP	DODAP	Chol	$Cer_{16}PEG_{2000}$
M1	94 mol%	–	–	6 mol%
M2	34 mol%	–	62 mol%	4 mol%
M3	34 mol%	31 mol%	31 mol%	4 mol%
M4	47 mol%	47 mol%	–	6 mol%

miRNA aqueous solution with the CaP nanoparticles in a 1:9 v/v ratio; the suspension was vortexed and incubated at room temperature for 10 min. The CaP-miRNA mixture was then added to the liposomes in a 1:1 v/v ratio and incubated at room temperature for 25 min to obtain miRNA-loaded SANP. The miRNA concentration in the final formulation was 200 μg/mL. The concentration of encapsulated miRNA was determined by measuring the amount of unencapsulated miRNA *via* the Quant-iT RiboGreen RNA Assay. The miRNA encapsulation efficiency was determined as:

$$\text{Encapsulation efficiency } (\%) = \frac{[miRNA]_{total} - [miRNA]_{buffer}}{[miRNA]_{total}} * 100,$$

where $[miRNA]_{total}$ is the total miRNA concentration in the formulation and $[miRNA]_{buffer}$ is the concentration of unencapsulated miRNA.

2.5. Nanoparticle physico-chemical characterization

The formulations were characterized in terms of colloidal dimensions, polydispersity index (PDI), and surface charge by using dynamic light scattering (DLS) (Zetasizer Nano Z, Malvern, UK). For each formulation the z-average diameter, PDI, and zeta potential were calculated as mean ± standard deviation of measurements from N = 2 independent batches.

2.6. Stability of miRNA-SANP formulations in biological media

The stability against aggregation of miRNA-SANP formulations upon dilution in human plasma was measured *via* DLS. Blood was first centrifuged at 2000 rpm for 15 min (MIKRO 20; Hettich, Tuttlingen, Germany) to separate the erythrocytes from the plasma, which was diluted at 1 % and 10 % v/v in phosphate buffer (136 mM NaCl, 27 mM KCl, 8 mM Na_2HPO_4, 2 mM KH_2PO_4, 1X PBS) at pH 7.4. MiRNA-SANP formulations were incubated in a 1 % or 10 % plasma solution at 37 °C at a final concentration of 20 μg/mL and the mean hydrodynamic diameter of the formulations was measured at various time points by DLS. MiRNA-SANP incubated in PBS were used as controls.

2.7. Hemolysis assay

Hemolysis assays on miRNA-SANP formulations were performed on fresh blood as previously reported [22]. Briefly, the erythrocytes were separated from the plasma by centrifugation at 2000 rpm for 15 min (MIKRO 20; Hettich, Tuttlingen, Germany) and then reconstituted in 150 mM NaCl solution. Reconstituted erythrocytes were subjected to three more centrifugation and reconstitution steps to remove residual plasma and then diluted 1:10 v/v in 150 mM NaCl. MiRNA-SANP formulations were added to the erythrocytes at 0.2 % w/v and incubated at 37 °C for 4 h. The samples were then placed on ice for 2 min to stop erythrocytes lysis and centrifuged twice (3000 rpm, 5 min) to retrieve the supernatant. The free hemoglobin content was determined by measuring the absorbance of the supernatants at 540 nm (Thermo Fisher Scientific 1510 Multiskan Go). Erythrocytes diluted in 150 mM NaCl or water were used as the 0 % and 100 % hemolysis controls, respectively. The hemolysis percentage was calculated by using the following formula:

$$Hemolysis\ \% = \frac{(Abs_{sample} - Abs_{0\%})}{(Abs_{100\%} - Abs_{0\%})} * 100,$$

where Abs_{sample} is the absorbance of the sample, $Abs_{0\%}$ is the absorbance of the sample at 0 % hemolysis, and $Abs_{100\%}$ is the absorbance of the sample at 100 % hemolysis.

2.8. Cell lines and treatments

BRAF-mutated melanoma cell lines A375, M14 and WM266 were purchased from American Type Culture Collection (ATCC, Manassas, VA, USA). A375 double resistant cells (DR) have been selected in the presence of both BRAF and MEK inhibitors as describe above (Fattore et al., Oncogene 2022). All human melanoma cell lines were cultured in RPMI (complete medium) supplemented with 10 % (vol/vol) FBS, L-glu at 2 % (vol/vol) and Pen-Strep at 1 % (vol/vol). Dabrafenib and trametinib as BRAFi and MEKi, respectively, were obtained by Novartis Farma S.p.A. (Rome, Italy). For biological assay, dabrafenib was used at decreasing concentrations starting from 1 μm and then diluted 1:3 for ten times. Trametinib was used in a ratio 1:10 as compared to Dabrafenib and diluted 1:3 for ten times. The number of viable melanoma cells was measured by quantification of the ATP present according to CellTiter-Glo® Luminescent Cell Viability assay protocol. Colony formation assays have been performed by crystal violet staining upon exposure of melanoma cells to SANP-SCR or SANP-miRs for 72 h. Briefly, the cells were stained for 20 min at room temperature with staining solution (0, 5 % crystal violet in 30 % methanol), washed four times with water and then dried. Cells were then dissolved in 10 % acetic acid solution and the absorbance (595 nm) was read using a microplate ELISA reader.

2.9. Elisa assays

Soluble VEGFA and TGFβ1 levels from melanoma cell media were determined by measuring absorbance at 450 nm into a microplate reader using specific ELISA kit according to the manufacturer's instructions. In particular, VEGFA kit (#DVE00) was purchased by the R&D system (Minneapolis, MN USA) whereas TGFβ1 kit (#EH0287) was purchased by the FineTest (Wuhan, China).

2.10. RNA extraction and quantitative real time PCR (qRT-PCR) analysis

Total RNA was extracted using TRIzol according to the manufacturer's instruction and quantitated by the Qubit Fluorometer (ThermoFisher Scientific, Foster City, CA, USA). RNA was retrotranscribed using the kit OneScript Plus cDNA Synthesis Kit (Abm, Richmond, BC, Canada) according to manufacturer's instruction. The cDNAs obtained, were adequately diluted in DEPC-H_2O. Following, 25 ng of cDNA were used to analyze the expression of miR-204–5p, miR-199b-5p, and U6 through quantitative real-time PCR using TaqMan Expression Assays (ThermoFisher Scientific). The results were evaluated by the ΔΔCt method.

2.11. Statistical analysis

Experiments were replicated at least three times and the data were expressed as average ± SD of the mean (SEM). Differences between groups were analyzed with a two-tailed paired or unpaired Student's t-test and were considered statistically significant for p-value <0.05. To evaluate the results of the combinations of SANPs + MAPKi, quantitative analysis for curve fitting and p-value estimation (significance $p < 0.05$) were performed by GraphPad Prism 7 (San Diego, CA, USA).

3. Results and discussion

3.1. Design and characterization of miRNA-SANP formulations

MiRNA-loaded SANP can be obtained by mixing liposomes, calcium phosphate nanoparticles, and miRNA (Fig. 1a). We investigated various lipid compositions for the formulation of miRNA-loaded SANP (Table 1) to elucidate the effect of cholesterol and of an ionizable lipid on the efficacy of the formulation. In particular, we used 1,2-dioleoyl-3-trimethylammoniumpropane (DOTAP) and $Cer_{16}PEG_{2000}$ as the cationic and the PEGylated lipid, respectively. DOTAP is a permanent cationic lipid

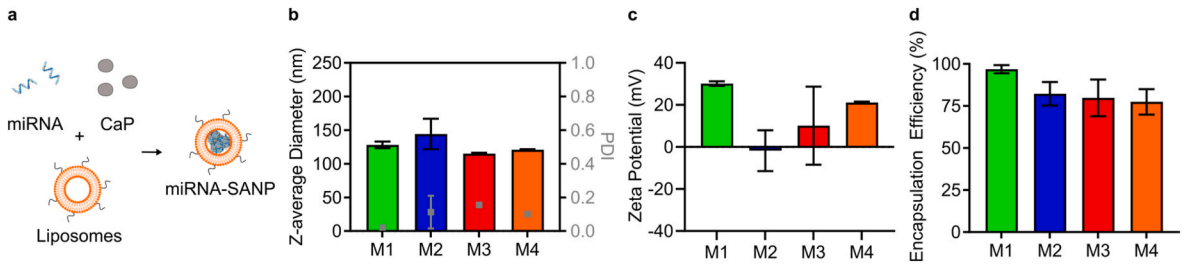

Fig. 1. (a) Schematic of miRNA-loaded SANP, which can be obtained by mixing miR-199b-5p, the CaP nanoparticles, and the liposomes. miRNA-SANP formulations were characterized in terms of hydrodynamic diameter and polydispersity index (b), zeta potential (c), and miRNA encapsulation efficiency (d). Data is shown as mean ± s.d. of N = 2 independent batches.

and has been extensively used for the formulation of cationic lipid-based nanoparticles for nucleic acid delivery [27]; DOTAP-based SANP formulations outperformed SANP based on other common cationic lipids such as N-[1-(2,3-dioleyloxy)propyl]-N,N,N-trimethylammonium chloride (DOTMA) and 3β-[N-(N′,N′-dimethylaminoethane)-carbamoyl] cholesterol hydrochloride (DC-chol) in terms of colloidal stability in serum, hemolytic activity, and cell viability [22]. Furthermore, we have previously observed enhanced miRNA delivery from SANP when $Cer_{16}PEG_{2000}$ was used as the PEGylated lipid compared to 1,2-distearoyl-sn-glycero-3-phosphoethanolamine-N-[amino(polyethylene glycol)-2000] ($DSPE\text{-}PEG_{2000}$), which may be ascribed to the tendency of $Cer_{16}PEG_{2000}$ to favor hexagonal phases in lipid-based nanoparticles [22,29]. The lipid composition of the M1 and M2 formulations has been shown to successfully deliver miRNA for the treatment of glioblastoma [22]; here, we decided to include a well-known ionizable lipid such as DODAP in the lipid composition of SANP to investigate its efficacy in combination with DOTAP.

We prepared miRNA-loaded SANP to a final miRNA concentration of 200 μg/mL and we characterized the formulations in terms of colloidal properties and miRNA encapsulation efficiency. MiRNA-loaded SANP formulations exhibited hydrodynamic diameters below 150 nm and PDI <0.2, regardless of the lipid composition (Fig. 1b); complexation with the CaP nanoparticles and miRNA resulted in minimal changes in the hydrodynamic diameter of the formulations compared to the starting liposomes (Table 2), as previously observed [22]. The zeta potential was higher than 20 mV for the M1 and M4 SANP formulations while it was near neutral for the cholesterol-containing formulations M2 and M3 (Fig. 1c). We observed a reduction in the zeta potential for all the miRNA-SANP formulations compared to the starting liposomes (Table 2), which suggests that the negatively charged miRNA interacts with the cationic lipids. The near neutral surface charge of the cholesterol-containing formulations M2 and M3 SANP may also suggest that the miRNA localizes on the outer shell of the nanoparticles as a result of lipid reorganization induced by cholesterol.

The miRNA encapsulation efficiency was ≥77 % across all the formulations, with the M1 SANP formulation exhibiting the highest encapsulation efficiency (97 %) (Fig. 1d). Variations in the colloidal properties and the miRNA encapsulation efficiency of SANP formulations may be due to differences in their lipid composition, which can affect the bilayer properties of the liposomes. For example, we have recently observed that the bilayer of DOTAP-$Cer_{16}PEG_{2000}$ liposomes features DOTAP- and $Cer_{16}PEG_{2000}$-enriched domains and that the inclusion of cholesterol in their composition facilitates lipid mixing [30]. In turn, the bilayer properties of the liposomes can affect the structural re-organization of the components upon SANP formation and the extent of miRNA complexation.

Table 2
Z-average diameter and PDI of the liposomes used for the formulation of miRNA-loaded SANP. Data is shown as mean ± s.d. of N = 2–3 independent batches.

Liposomal Formulation	Z-average Diameter (nm)	PDI	Zeta Potential (mV)
M1	135.8 ± 1.1	0.06 ± 0.03	30.8 ± 18.9
M2	124.4 ± 5.6	0.04 ± 0.01	43.2 ± 2.5
M3	108.4 ± 7.2	0.16 ± 0.01	55.1 ± 0.1
M4	118.4 ± 3.7	0.13 ± 0.01	45.6 ± 8.7

3.2. *Colloidal stability in biological fluids and hemolytic activity of miRNA-SANP formulations*

Since miRNA-SANP formulations have been designed for intravenous administration, we characterized their colloidal stability against aggregation upon dilution in either 1 % and 10 % v/v serum. We incubated miRNA-SANP formulations in the presence of serum at 37 °C and measured the mean hydrodynamic diameter at different time points, namely immediately after dilution and 1 and 4 h post-dilution. MiRNA-SANP formulations incubated in PBS were used as a control. No major changes in the hydrodynamic diameter could be observed for all the formulations in the presence of 1 % v/v serum compared to the control (Fig. 2a–d); the mean hydrodynamic diameter increased over time for the M1 and M2 SANP formulations in the presence of 10 % v/v serum (Fig. 2a and b). This behaviour was particularly clear for the M1 SANP formulation, whose mean hydrodynamic diameter increased by 30 nm over 4 h, which may be indicative of an extensive adsorption of serum proteins on the nanoparticle surface.

The mean hydrodynamic diameter of DODAP-containing SANP formulations remained unchanged even in the presence of 10 % v/v serum (**Figure c-d**), suggesting that these formulations exhibited a reduced serum protein adsorption. The role of ionizable lipids in the adsorption of serum protein on the surface of lipid nanoparticles has become increasingly clear and dictates their *in vivo* fate. It has been shown that the adsorption of apolipoprotein E on the surface of lipid nanoparticles allowed the preferential uptake of the nanoparticles by hepatocytes and facilitated RNA delivery to the liver [31]. It is possible that in the presence of DODAP there is a reduced interaction between the nanoparticle surface and serum proteins. While the role of ionizable lipids on the protein corona formation in LNPs is well-established [32–34], ongoing studies in our group are investigating the effect of the lipid SANP composition on serum protein adsorption.

We also measured the hemolytic activity of miRNA-SANP formulations in human blood to investigate whether they could be administered intravenously without inducing severe systemic toxicity. A hemolytic activity <2 % or comprised between 2 and 5 % were regarded as non-toxic or mildly toxic, respectively. All the tested miRNA-SANP formulations exhibited a hemolytic activity below 1.6 (Table 3), which suggests that the formulations are not toxic for red blood cells and can be administered *via* intravenous injection.

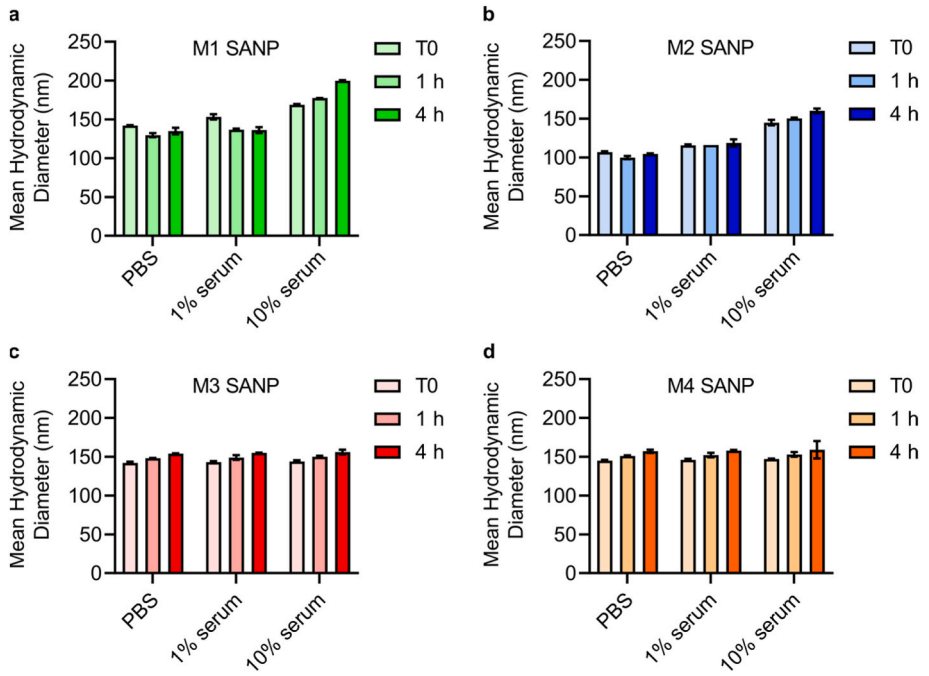

Fig. 2. Colloidal stability of M1 SANP (a), M2 SANP (b), M3 SANP (c), and M4 SANP (d) loaded with miR-199b-5p and diluted to 20 μg/mL miRNA in either PBS, 1 % v/v serum, or 10 % v/v serum; the formulations were incubated at 37 °C and the hydrodynamic diameter was measured immediately after dilution and 1 and 4 h post-dilution. Measurements were carried out in duplicate.

Table 3
Hemolytic activity of miRNA-SANP formulations. Data is shown as mean ± s. d. of N = 3 independent experiments.

miRNA-SANP Formulations	Hemolytic Activity (%)
M1 SANP	1.44 ± 0.93
M2 SANP	1.08 ± 0.41
M3 SANP	1.59 ± 1.05
M4 SANP	1.60 ± 1.06

3.3. *In vitro cytotoxicity of SANP formulations on BRAF-mutant human melanoma cells*

We then carried out *in vitro* studies using BRAF-mutant melanoma cell lines as a model system. To this purpose, we decided to test SANPs cytotoxicity *in vitro* in the absence of therapeutic miRNA cargos. A375 melanoma cell were exposed for 72 h to different concentrations (1, 5, 10 or 20 μg/mL) of M1, M2, M3 or M4 SANPs containing either the scrambled miRNA sequence (SCR). Cell viability was tested by measuring cellular ATP by luminescence assays to determine metabolic activity in response to the exposure to SANP formulations. Results clearly indicated that the all the 4 SANP formulations tested had no significant impact on cell viability (Fig. 3a–d).

We then started to evaluate the biological and molecular impact of miRNA cargos delivered by SANP formulations on melanoma cell behavior. First of all, we tested the capability of SANP formulations to affect A375 cell proliferation. To this aim, we exposed cells to different concentrations of M1, M2, M3, and M4 SANPs delivering SCR or the oncosuppressive miR-204–5p for 72 h. Results demonstrated that M1 and M2 formulations carrying miR-204–5p were able to reduce melanoma cell proliferation as compared to SCR-loaded SANPs. Differently, M3 and M4 SANPs delivering miR-204–5p were not able to affect melanoma cell viability as compared to SANP-SCR. Interestingly, an equivalent anti-proliferative effect on A375 cells has been obtained with 5 or with 20 μg/mL of miRNA delivered by M1 or M2 SANPs (Fig. 4, upper panels).

In line with this, we demonstrated that M1 and M2 SANPs were able to induce the intracellular uptake of miR-204–5p at a similar degree of magnitude at both concentrations (5 vs 20 μg/mL) (Supplementary Fig. 1). Given these results, we decided to use M1 and M2 SANPs and 5 μg/mL of miRNAs for the following biological experiments.

3.4. *SANP formulations induce miR-204–5p/miR-199b-5p uptake and inhibit their target genes*

Given the results of the previous paragraph on miR-204–5p, we decided to test the ability of M1 and M2 SANPs to effectively deliver combinations of oncosuppressive miRNAs (i.e., miR-204–5p and miR-199b-5p, briefly SANP-miRs) in various melanoma cell lines. The rationale of this approach lies on our previous data demonstrating that miRNA combinations, delivered by LNPs, are able to better reduce melanoma cell proliferation as compared to single miRNAs [12]. This relies on their capability to simultaneously hit multiple oncogenic signaling [12,13]. Therefore, we exposed A375 cells to M1 or M2 SANPs encapsulating miR-204–5p and miR-199b-5p for 72 h. Based on the results of the previous paragraph, we used 5 μg/mL of total miRNAs (50 % of miR-204–5p + 50 % of miR-199b-5p) for these experiments. First of all, qRT-PCR experiments showed that both M1 and M2 formulations were able to efficiently induce miR-204–5p/miR-199b-5p uptake in A375 and M14 melanoma cells (Fig. 5a and b and Supplementary Fig. 2).

Moreover, in order to test whether miRNA uptake was effectively able to reduce the levels of given target genes, we have tested the levels of TGFβ1 and VEGFA, which are molecular targets of miR-204–5p and miR-199b-5p, respectively [13]. Given that these growth factors are released in cell media (CM), we collected CM from A375 cells following 72 h of exposure to M1 and M2 SANP-miRs to perform ELISA assays. Results clearly demonstrated that SANP-induced miRNA intracellular uptake was able to effectively reduce in parallel the levels of VEGFA and TGFβ1, as compared to SANP-SCR controls (Fig. 5c and d).

3.5. *SANP-miRs reduce melanoma cell growth per se and potentiate targeted therapies*

Finally, we sought to test the growth inhibitory effects of M1 and M2

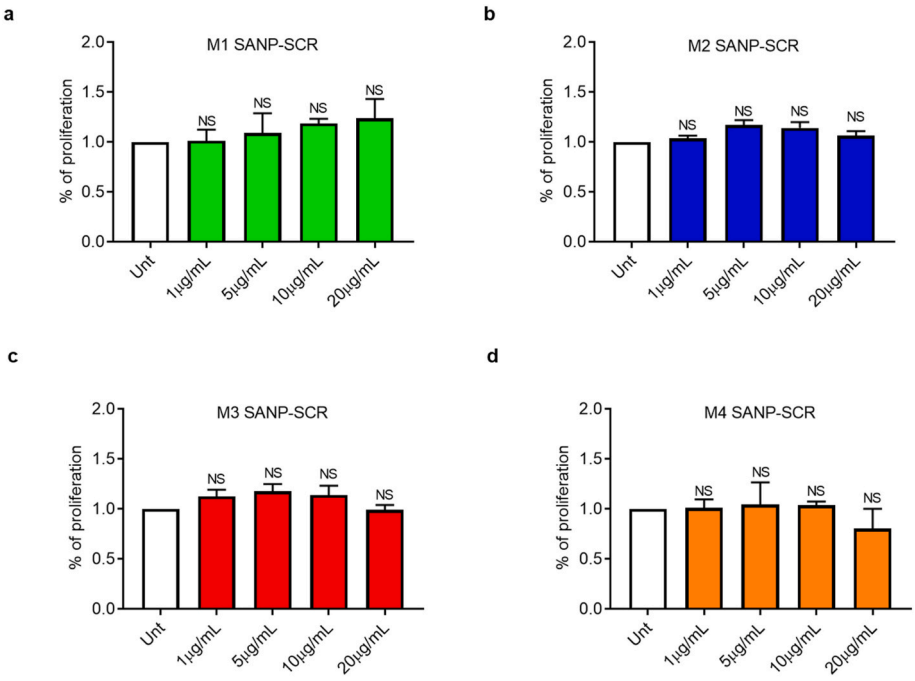

Fig. 3. *In vitro* cytotoxicity on A375 cell line exposed to M1 SANP (a), M2 SANP (b), M3 SANP (c), or M4 SANP (d) loaded with different concentrations of the scrambled sequences (SCR; 1, 5, 10 or 20 μg/mL). The formulations were prepared as previously described. Cell viability was measured after 72 h by quantification of the ATP present using CellTiter-Glo® Luminescent Cell Viability assay. The values were calculated as "fold change" (±S.D.) as compared to Unt cells. All the experiments have been performed at least in triplicate and p-value <0.05 was considered as significant (Student's t-test).

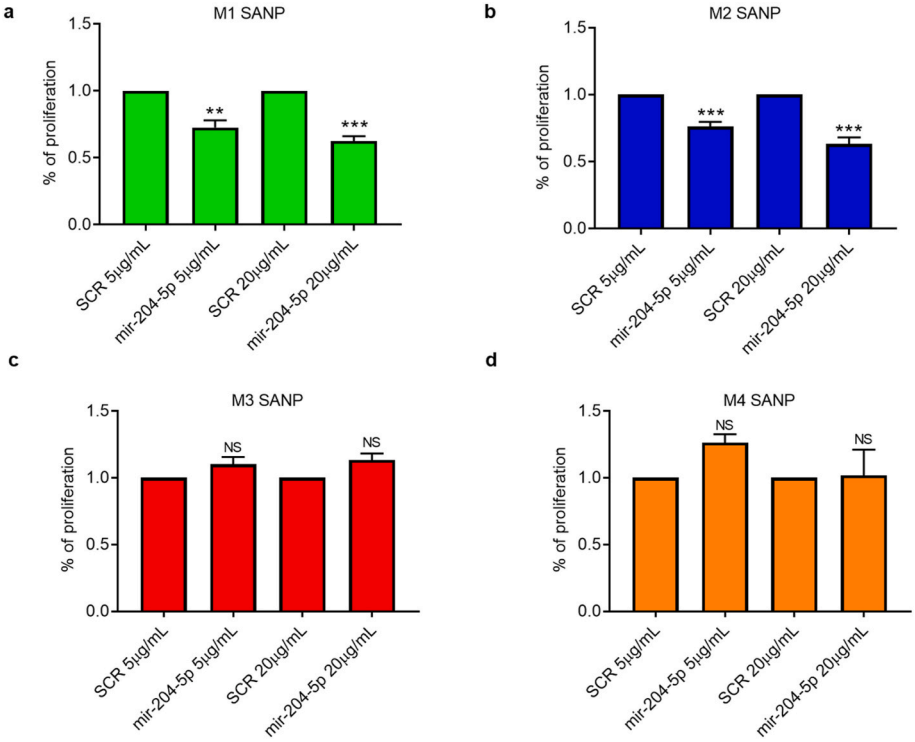

Fig. 4. *In vitro* cytotoxicity on A375 cell line exposed to M1 SANP (a), M2 SANP (b), M3 SANP (c), or M4 SANP (d) loaded with different concentrations of the scrambled sequences (SCR) or miR-204–5p (5 or 20 μg/mL). The formulations were prepared as previously described. Cell viability was measured after 72 h by quantification of the ATP present using CellTiter-Glo® Luminescent Cell Viability assay. The values were calculated as "fold change" (±S.D.) as compared to cells receiving SANP-SCR.

SANPs delivering miR-204–4p and miR-199b-5p alone or in combination with BRAF and MEK inhibiting drugs. First of all, we exposed A375 and M14 melanoma cell lines to SANP-miRs for 72 h to evaluate cell viability, as previously described. Results clearly demonstrated that both these M1 and M2 formulations were able to reduce melanoma cell proliferation as compared to SANPs carrying SCR sequences, used as

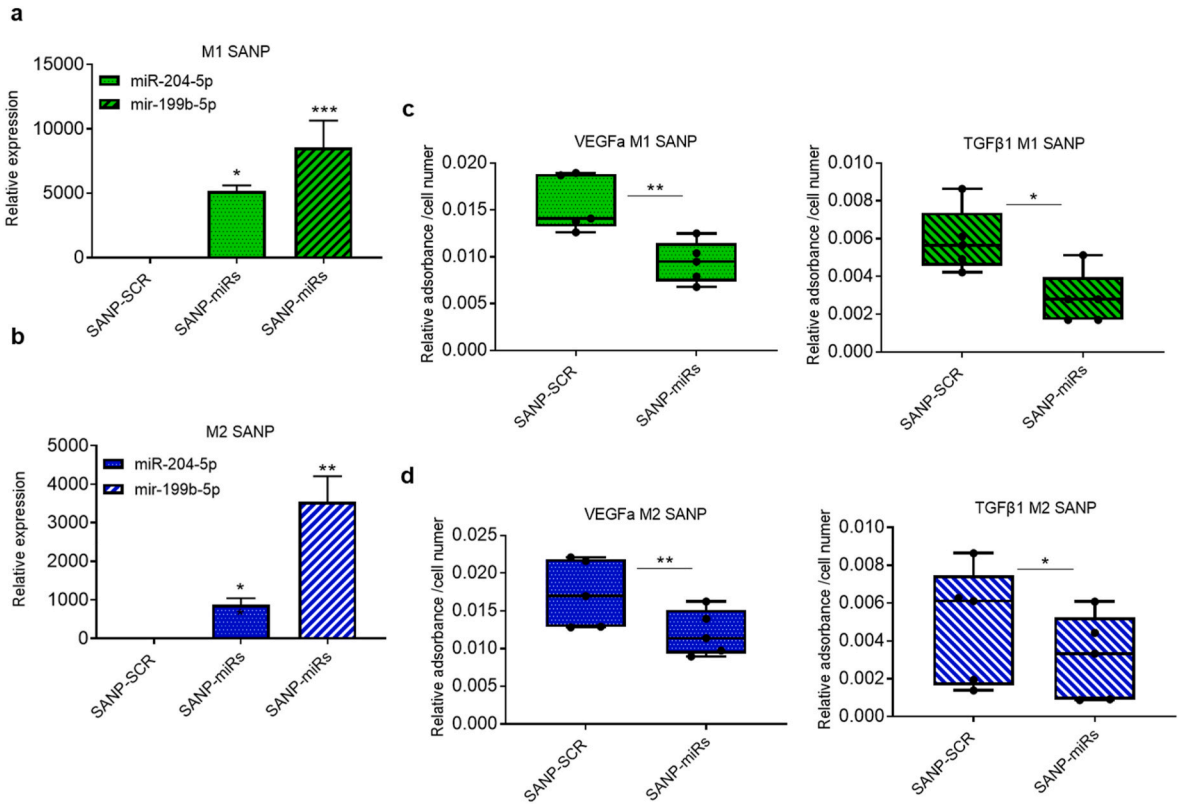

Fig. 5. A375 cell line was exposed to 5 μg/mL of M1 SANP-SCR or SANP-miRs (a) and M2 SANP-SCR or SANP-miRs (b) for 72 h. The formulations were prepared as previously described. Total RNA was extracted to perform qRT-PCR on the expression levels of the indicated miRNAs. Results were normalized by DDCT method relative to U6. The values were calculated as "fold change" (±S.D.) as compared to cells receiving SANP-SCR. Elisa assays were performed to measure VEGFA and TGFβ1 in cell media (CM) deriving from A375, exposed to M1 SANP-SCR or SANP-miRs (c) and M2 SANP-SCR or SANP-miRs (d) for 72 h. For these experiments cells have been serum starved for 24 h and then CM have been collected; results were determined by measuring absorbance at 450 nm into a microplate reader. All the experiments have been performed at least in triplicate and p-value <0.05 was considered as significant (Student's t-test).

control (Fig. 6a and b). Of note, the same findings were obtained in two additional melanoma cell lines, namely WM266 and A375DR, which is a cell line, derived from A375 cells, rendered double resistant to both BRAFi/MEKi (Supplementary Fig. 3). These data have been further confirmed through colony formation assays. For these experiments, A375 and M14 melanoma cells have been exposed for 72 h to M1 or M2 SANP-miRs or SANP-SCR, and then cells have been collected and plated at low density (i.e. 1000 cells/well). Results obtained by crystal violet staining confirm that both the formulations delivering the oncosuppressive miRs are able to reduce the clonogenic capability of both A375 and M14 melanoma cells (Supplementary Figs. 4 and 5).

Once determined the effects on tumor cell proliferation *per se,* we investigated whether SANP-miRs could be able to potentiate targeted therapies. To this aim, we combined M1 or M2 SANP-miRs or SANP-SCR with different concentrations of BRAFi and MEKi for 72 h to evaluate melanoma cell viability, as previously described. Results clearly show that the both SANP formulations carrying oncosuppressive miR-204–5p and miR-199b-5p were able to potentiate targeted therapies growth inhibitory effects in both A375 and M14 cell lines (Fig. 6c and d). Altogether these findings suggest the possibility that SANPs carrying a combination of oncosuppressor miRNAs may be novel therapeutic tools towards precision medicine for BRAF-mutant melanomas not only *per se* but also when combined with BRAF and MEK inhibiting drugs.

4. Conclusions

In the last few years, the transition of RNA-based therapeutics to the clinical practice in oncology has dramatically accelerated thanks to the success in the fight against the SARS-CoV2 pandemic of LNP-based vaccines. This is the case of mRNA-4157, a mRNA-based individualized neoantigen vaccine encapsulated in LNPs whose efficacy has been demonstrated in a phase 2b clinical trial in combination with immunotherapy in patients with advanced melanoma [35]; based on these results, a phase 3 study has been initiated (ClinicalTrials.gov identifier: NCT05933577). The transition to the clinical practice of miRNA therapeutics seems to be more difficult, with clinical trials that have reported either fatal immune-related side effects [36] or dose-limiting toxicities alongside decreased lymphocyte counts and cardiac events [37]. Altogether, these studies suggest that more efforts are needed to make miRNAs suitable cancer therapeutics, in particular to improve delivery methods and to reduce unwanted toxicities.

In the context of BRAF-mutated melanoma, target therapy has greatly improved the survival rates of patients but its long-term efficacy is compromised by the onset of drug resistance. Our group has recently demonstrated that non-coding oligonucleotides such as miR-204–5p and miR-199b-5p can modulate resistance to MAPK inhibitors in metastatic melanoma [5,38] and could represent a promising strategy to potentiate the efficacy of these drugs. Here, we decided to leverage the lipid SANP technology to deliver a mixture of miR-204–5p and miR-199b-5p to melanoma cells in combination with MAPK inhibitors. SANP can be obtained by mixing CaP NPs, cationic liposomes, and miRNA directly at the point-of-care, an approach that would enable patient-centric nanomedicine formulation. We developed SANP formulations with varying lipid compositions with miRNA encapsulation efficiencies >75 %, good colloidal stability in serum, and low hemolytic activity. We selected two SANP formulations based on preliminary cell viability and miRNA uptake studies on BRAF-mutant human melanoma cells. These formulations were able to potentiate the growth inhibition effect of BRAF and

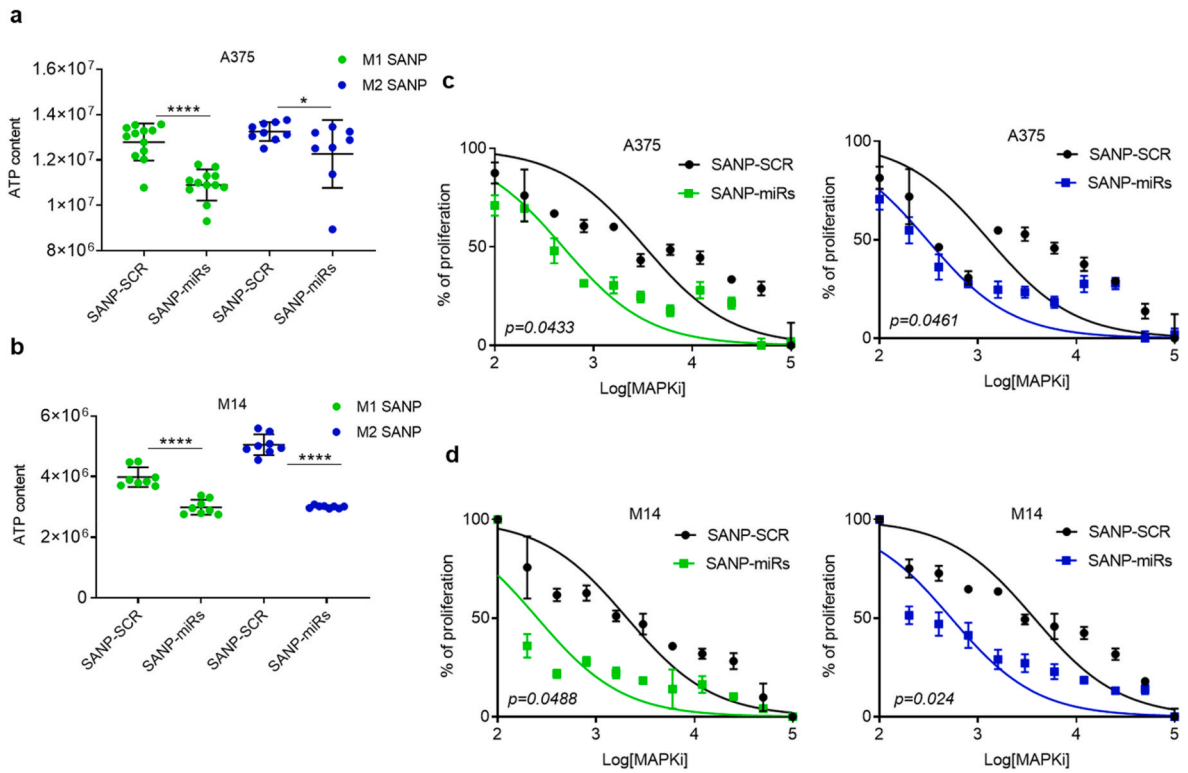

Fig. 6. Cell viability was determined measuring ATP content in A375 (a) and M14 (b) cell lines treated with 5 μg/mL of M1/M2 SANP-SCR or SANP-miRs for 72 h. The formulations were prepared as previously described. A375 (c) and M14 (d) cells were exposed to MAPKi, i.e dabrafenib (BRAFi) + trametinib (MEKi), in the presence of 5 μg/mL of M1/M2 SANP-SCR or SANP-miRs. Cell viability was determined after 72 h as previously described. Dabrafenib was used at decreasing concentrations starting from 1μM and then diluted 1:3 for ten times. Trametinib was used in a ratio 1:10 as compared to Dabrafenib and diluted 1:3 for ten times. The values were calculated as "fold change" (±S.D.) as compared to cells receiving SANP-SCR. All the experiments have been performed at least in triplicate and p-value <0.05 was considered as significant (Student's t-test). Quantitative analysis for curve fitting were performed by GraphPad Prism 7.

MEK inhibitors, which makes our approach a promising strategy to tackle drug resistance in metastatic melanoma. Future studies will be aimed at assessing the tolerability and efficacy of SANP-miRs in combination with MAPK inhibitors in *in vivo* models of melanoma.

In this work, we show for the first time the potential of a novel nanotechnological platform to deliver combinations of oncosuppressive miRNAs for the therapy of cancer. Data reported in this study support the versatility of SANP formulations, which can be tuned to maximize miRNA encapsulation and intra-cellular delivery in specific cells, such as metastatic melanoma cells. Moreover, the miRNA-SANP formulations developed in this study enable to overcome some of the limitations of LNP formulations in the context of long-term stability upon storage and personalized therapy. Overall, SANP-miRs exhibit high versatility and great potential for rapid clinical translation, as well as potential for personalized cancer therapy; we envision the development of an investigational medicinal product based on a kit comprising the miRNAs, a vial containing the liposomes, and a vial containing the CaP NPs. A similar kit approach was proposed for mRNA-loaded lipoplexes [39], which are now under investigation in various clinical trials as anti-cancer vaccines for melanoma [40] and pancreatic cancer [41]. The applicability of the lipid SANP technology extends beyond metastatic melanoma and can be rapidly translated to other cancer and disease models requiring oligonucleotide delivery.

CRediT authorship contribution statement

Valeria Nele: Writing – review & editing, Writing – original draft, Methodology, Investigation, Formal analysis, Data curation, Conceptualization. **Domenico Liguoro:** Methodology, Investigation, Formal analysis. **Virginia Campani:** Writing – review & editing, Visualization. **Alessia Angelillo:** Investigation. **Rachele Frigerio:** Methodology, Investigation, Formal analysis. **Arianna Ortolano:** Methodology, Investigation, Formal analysis. **Rita Mancini:** Writing – original draft, Supervision, Resources, Project administration, Funding acquisition, Conceptualization. **Luigi Fattore:** Writing – review & editing, Writing – original draft, Methodology, Formal analysis, Data curation, Conceptualization. **Giuseppe De Rosa:** Writing – original draft, Supervision, Resources, Project administration, Funding acquisition, Conceptualization. **Gennaro Ciliberto:** Writing – original draft, Supervision, Resources, Project administration, Funding acquisition, Conceptualization.

Declaration of competing interest

The authors declare that they have no known competing financial interests or personal relationships that could have appeared to influence the work reported in this paper.

Data availability

Data will be made available on request.

Acknowledgments

The study was supported by Italian Minister of University grant PRIN 2022 Prot. 2022L8H27T to Prof. Ciliberto and Prof. De Rosa. The study was also supported by Italian Minister of Health through the grant PNRR-POC-2022-12375713 to Prof. Ciliberto and by "PNRR M4C2-Investimento 1.4- CN00000041" from European Union-NextGenerationEU to Rita Mancini. V.N. was supported by Fondazione Umberto Veronesi Post-Doctoral Fellowship.

Appendix A. Supplementary data

Supplementary data to this article can be found online at https://doi.org/10.1016/j.jddst.2024.106169.

References

[1] F. Valenti, I. Falcone, S. Ungania, F. Desiderio, P. Giacomini, C. Bazzichetto, F. Conciatori, E. Gallo, F. Cognetti, G. Ciliberto, et al., Precision medicine and melanoma: multi-omics approaches to monitoring the immunotherapy response, Int. J. Mol. Sci. 22 (2021) 3837, https://doi.org/10.3390/ijms22083837.

[2] L. Kuryk, L. Bertinato, M. Staniszewska, K. Pancer, M. Wieczorek, S. Salmaso, P. Caliceti, M. Garofalo, From conventional therapies to immunotherapy: melanoma treatment in review, Cancers 12 (2020), https://doi.org/10.3390/cancers12103057.

[3] S. Kalaora, A. Nagler, J.A. Wargo, Y. Samuels, Mechanisms of immune activation and regulation: lessons from melanoma, Nat. Rev. Cancer (2022), https://doi.org/10.1038/s41568-022-00442-9.

[4] L. Fattore, S. Costantini, D. Malpicci, C.F. Ruggiero, P.A. Ascierto, C.M. Croce, R. Mancini, G. Ciliberto, MicroRNAs in melanoma development and resistance to target therapy, Oncotarget 8 (No 13) (2017).

[5] L. Fattore, C.F. Ruggiero, M.E. Pisanu, D. Liguoro, A. Cerri, S. Costantini, F. Capone, M. Acunzo, G. Romano, G. Nigita, et al., Reprogramming MiRNAs global expression orchestrates development of drug resistance in BRAF mutated melanoma, Cell Death Differ. 26 (2019) 1267–1282, https://doi.org/10.1038/s41418-018-0205-5.

[6] S.W.L. Lee, C. Paoletti, M. Campisi, T. Osaki, G. Adriani, R.D. Kamm, C. Mattu, V. Chiono, MicroRNA delivery through nanoparticles, J. Contr. Release 313 (2019) 80–95, https://doi.org/10.1016/j.jconrel.2019.10.007.

[7] R. Rupaimoole, F.J. Slack, MicroRNA therapeutics: towards a new era for the management of cancer and other diseases, Nat. Rev. Drug Discov. 16 (2017) 203–222, https://doi.org/10.1038/nrd.2016.246.

[8] Z. Bai, J. Wei, C. Yu, X. Han, X. Qin, C. Zhang, W. Liao, L. Li, W. Huang, Non-viral nanocarriers for intracellular delivery of MicroRNA therapeutics, J. Mater. Chem. B 7 (2019) 1209–1225, https://doi.org/10.1039/C8TB02946F.

[9] K. Gokita, J. Inoue, H. Ishihara, K. Kojima, J. Inazawa, Therapeutic potential of LNP-mediated delivery of MiR-634 for cancer therapy, Mol. Ther. Nucleic Acids 19 (2020) 330–338, https://doi.org/10.1016/j.omtn.2019.10.045.

[10] X. Huang, J. Magnus, V. Kaimal, P. Karmali, J. Li, M. Walls, R. Prudente, E. Sung, M. Sorourian, R. Lee, et al., Lipid nanoparticle–mediated delivery of anti-MiR-17 family oligonucleotide suppresses hepatocellular carcinoma growth, Mol. Cancer Therapeut. 16 (2017) 905–913, https://doi.org/10.1158/1535-7163.MCT-16-0613.

[11] M.T. Di Martino, V. Campani, G. Misso, M.E. Gallo Cantafio, A. Gullà, U. Foresta, P. H. Guzzi, M. Castellano, A. Grimaldi, V. Gigantino, et al., In vivo activity of MiR-34a mimics delivered by stable nucleic acid lipid particles (SNALPs) against multiple myeloma, PLoS One 9 (2014) e90005, https://doi.org/10.1371/journal.pone.0090005.

[12] L. Fattore, V. Campani, C.F. Ruggiero, V. Salvati, D. Liguoro, L. Scotti, G. Botti, P. A. Ascierto, R. Mancini, G. De Rosa, et al., In vitro biophysical and biological characterization of lipid nanoparticles Co-encapsulating oncosuppressors MiR-199b-5p and MiR-204-5p as potentiators of target therapy in metastatic melanoma, Int. J. Mol. Sci. 21 (2020) 1930, https://doi.org/10.3390/ijms21061930.

[13] L. Fattore, G. Cafaro, M. Di Martile, V. Campani, A. Sacconi, D. Liguoro, E. Marra, S. Bruschini, D. Stoppoloni, R. Cirombella, et al., Oncosuppressive MiRNAs loaded in lipid nanoparticles potentiate targeted therapies in BRAF-mutant melanoma by inhibiting core escape pathways of resistance, Oncogene 42 (2023) 293–307, https://doi.org/10.1038/s41388-022-02547-9.

[14] T. Ito, Y. Tanaka, M. Murata, Y. Kaku-Ito, K. Furue, M. Furue, BRAF heterogeneity in melanoma, Curr. Treat. Options Oncol. 22 (2021) 20, https://doi.org/10.1007/s11864-021-00818-3.

[15] V. Campani, S. Giarra, G. De Rosa, Lipid-based core-shell nanoparticles: evolution and potentialities in drug delivery, Open 3 (2018) 5–17, https://doi.org/10.1016/j.onano.2017.12.001.

[16] J. Li, Y.-C. Chen, Y.-C. Tseng, S. Mozumdar, L. Huang, Biodegradable calcium phosphate nanoparticle with lipid coating for systemic SiRNA delivery, J. Contr. Release 142 (2010) 416–421, https://doi.org/10.1016/j.jconrel.2009.11.008.

[17] A.-Y. Cai, Y.-J. Zhu, C. Qi, Biodegradable inorganic nanostructured biomaterials for drug delivery, Adv. Mater. Interfac. 7 (2020) 2000819, https://doi.org/10.1002/admi.202000819.

[18] G. Salzano, M. Marra, M. Porru, S. Zappavigna, A. Abbruzzese, M.I. La Rotonda, C. Leonetti, M. Caraglia, G. De Rosa, Self-assembly nanoparticles for the delivery of bisphosphonates into tumors, Int. J. Pharm. 403 (2011) 292–297, https://doi.org/10.1016/j.ijpharm.2010.10.046.

[19] M. Marra, G. Salzano, C. Leonetti, M. Porru, R. Franco, S. Zappavigna, G. Liguori, G. Botti, P. Chieffi, M. Lamberti, et al., New self-assembly nanoparticles and stealth liposomes for the delivery of zoledronic acid: a comparative study, Biotechnol. Adv. 30 (2012) 302–309, https://doi.org/10.1016/j.biotechadv.2011.06.018.

[20] M. Abate, L. Scotti, V. Nele, M. Caraglia, M. Biondi, G. De Rosa, C. Leonetti, V. Campani, S. Zappavigna, M. Porru, Hybrid self-assembling nanoparticles encapsulating zoledronic acid: a strategy for fostering their clinical use, Int. J. Mol. Sci. 23 (2022) 5138, https://doi.org/10.3390/ijms23095138.

[21] M. Porru, S. Zappavigna, G. Salzano, A. Luce, A. Stoppacciaro, M.L. Balestrieri, S. Artuso, S. Lusa, G. De Rosa, C. Leonetti, et al., Medical treatment of orthotopic glioblastoma with transferrin-conjugated nanoparticles encapsulating zoledronic acid, Oncotarget 5 (21) (2014) 10446, https://doi.org/10.18632/oncotarget.2182.

[22] V. Campani, S. Zappavigna, L. Scotti, M. Abate, M. Porru, C. Leonetti, M. Caraglia, G. De Rosa, Hybrid lipid self-assembling nanoparticles for brain delivery of MicroRNA, Int. J. Pharm. 588 (2020) 119693, https://doi.org/10.1016/j.ijpharm.2020.119693.

[23] V. Nele, V. Tedeschi, V. Campani, R. Ciancio, A. Angelillo, S.F. Graziano, G. De Rosa, A. Secondo, Cerium-doped self-assembling nanoparticles as a novel anti-oxidant delivery system preserving mitochondrial function in cortical neurons exposed to ischemia-like conditions, Antioxidants 12 (2023), https://doi.org/10.3390/antiox12020358.

[24] V. Nele, S. Melini, V. Campani, A. Angelillo, S.F. Graziano, C. Pirozzi, R. Meli, G. De Rosa, Self-assembling nanoparticles with antioxidant activity for ROS scavenging in liver cells, J. Drug Deliv. Sci. Technol. 94 (2024) 105490, https://doi.org/10.1016/j.jddst.2024.105490.

[25] G. Derosa, D. Stefano, V. Laguardia, S. Arpicco, V. Simeon, R. Carnuccio, E. Fattal, Novel cationic liposome formulation for the delivery of an oligonucleotide decoy to NF-κb into activated macrophages, Eur. J. Pharm. Biopharm. 70 (2008) 7–18, https://doi.org/10.1016/j.ejpb.2008.03.012.

[26] E.S. Hosseini, M. Nikkhah, S. Hosseinkhani, <p>Cholesterol-Rich lipid-mediated nanoparticles boost of transfection efficiency, utilized for gene editing by CRISPR-cas9</P&gt, Int. J. Nanomed. 14 (2019) 4353–4366, https://doi.org/10.2147/IJN.S199104.

[27] Y. Zhang, C. Sun, C. Wang, K.E. Jankovic, Y. Dong, Lipids and lipid derivatives for RNA delivery, Chem. Rev. 121 (2021) 12181–12277, https://doi.org/10.1021/acs.chemrev.1c00244.

[28] R.A. Meyer, G.P. Hussmann, N.C. Peterson, J.L. Santos, A.D.A. Tuesca, Scalable and robust cationic lipid/polymer hybrid nanoparticle platform for MRNA delivery, Int. J. Pharm. 611 (2022) 121314, https://doi.org/10.1016/j.ijpharm.2021.121314.

[29] F. Shi, L. Wasungu, A. Nomden, M.C.A. Stuart, E. Polushkin, J.B.F.N. Engberts, D. Hoekstra, Interference of poly(ethylene glycol)–lipid analogues with cationic-lipid-mediated delivery of oligonucleotides; role of lipid exchangeability and non-lamellar transitions, Biochem. J. 366 (2002) 333–341, https://doi.org/10.1042/bj20020590.

[30] V. Nele, F. D'Aria, V. Campani, T. Silvestri, M. Biondi, C. Giancola, G. De Rosa, Unravelling the role of lipid composition on liposome-protein interactions, J. Liposome Res. (2023) 1–9, https://doi.org/10.1080/08982104.2023.2224449.

[31] A. Akinc, M.A. Maier, M. Manoharan, K. Fitzgerald, M. Jayaraman, S. Barros, S. Ansell, X. Du, M.J. Hope, T.D. Madden, et al., The Onpattro story and the clinical translation of nanomedicines containing nucleic acid-based drugs, Nat. Nanotechnol. 14 (2019) 1084–1087, https://doi.org/10.1038/s41565-019-0591-y.

[32] K. Liu, R. Nilsson, E. Lázaro-Ibáñez, H. Duàn, T. Miliotis, M. Strimfors, M. Lerche, A.R. Salgado Ribeiro, J. Ulander, D. Lindén, et al., Multiomics analysis of naturally efficacious lipid nanoparticle coronas reveals high-density lipoprotein is necessary for their function, Nat. Commun. 14 (2023) 4007, https://doi.org/10.1038/s41467-023-39768-9.

[33] M. Debnath, J. Forster, A. Ramesh, A. Kulkarni, Protein corona formation on lipid nanoparticles negatively affects the NLRP3 inflammasome activation, Bioconjugate Chem. 34 (2023) 1766–1779, https://doi.org/10.1021/acs.bioconjchem.3c00329.

[34] L. Miao, J. Lin, Y. Huang, L. Li, D. Delcassian, Y. Ge, Y. Shi, D.G. Anderson, Synergistic lipid compositions for albumin receptor mediated delivery of MRNA to the liver, Nat. Commun. 11 (2020) 2424, https://doi.org/10.1038/s41467-020-16248-y.

[35] J.S. Weber, M.S. Carlino, A. Khattak, T. Meniawy, G. Ansstas, M.H. Taylor, K. B. Kim, M. McKean, G.V. Long, R.J. Sullivan, et al., Individualised neoantigen therapy MRNA-4157 (V940) plus pembrolizumab versus pembrolizumab monotherapy in resected melanoma (KEYNOTE-942): a randomised, phase 2b study, Lancet 403 (2024) 632–644, https://doi.org/10.1016/S0140-6736(23)02268-7.

[36] D.S. Hong, Y.-K. Kang, M. Borad, J. Sachdev, S. Ejadi, H.Y. Lim, A.J. Brenner, K. Park, J.-L. Lee, T.-Y. Kim, et al., Phase 1 study of MRX34, a liposomal MiR-34a mimic, in patients with advanced solid tumours, Br. J. Cancer 122 (2020) 1630–1637, https://doi.org/10.1038/s41416-020-0802-1.

[37] N. van Zandwijk, N. Pavlakis, S.C. Kao, A. Linton, M.J. Boyer, S. Clarke, Y. Huynh, A. Chrzanowska, M.J. Fulham, D.L. Bailey, et al., Safety and activity of MicroRNA-loaded minicells in patients with recurrent malignant pleural mesothelioma: a first-in-man, phase 1, open-label, dose-escalation study, Lancet Oncol. 18 (2017) 1386–1396, https://doi.org/10.1016/S1470-2045(17)30621-6.

[38] L. Fattore, R. Mancini, M. Acunzo, G. Romano, A. Laganà, M.E. Pisanu, D. Malpicci, G. Madonna, D. Mallardo, M. Capone, et al., MiR-579-3p controls melanoma progression and resistance to target therapy, in: Proceedings of the National Academy of Sciences vol. 113, 2016, https://doi.org/10.1073/pnas.1607753113.

[39] S. Grabbe, H. Haas, M. Diken, L.M. Kranz, P. Langguth, U. Sahin, Translating nanoparticulate-personalized cancer vaccines into clinical applications: case study with RNA-lipoplexes for the treatment of melanoma, Nanomedicine 11 (2016) 2723–2734, https://doi.org/10.2217/nnm-2016-0275.

[40] U. Sahin, P. Oehm, E. Derhovanessian, R.A. Jabulowsky, M. Vormehr, M. Gold, D. Maurus, D. Schwarck-Kokarakis, A.N. Kuhn, T. Omokoko, et al., An RNA vaccine drives immunity in checkpoint-inhibitor-treated melanoma, Nature 585 (2020) 107–112, https://doi.org/10.1038/s41586-020-2537-9.

[41] L.A. Rojas, Z. Sethna, K.C. Soares, C. Olcese, N. Pang, E. Patterson, J. Lihm, N. Ceglia, P. Guasp, A. Chu, et al., Personalized RNA neoantigen vaccines stimulate T cells in pancreatic cancer, Nature 618 (2023) 144–150, https://doi.org/10.1038/s41586-023-06063-y.